EPE and Speed Adaptive Extended Kalman Filter for Vehicle Position and Attitude Estimation with Low Cost GNSS and IMU Sensors

(Draft)

t.b.d. t.b.d. t.b.d.
t.b.d. t.b.d. t.b.d.
t.b.d. t.b.d. t.b.d.

***Abstract*—This paper presents a novel approach for an adaptive Extended Kalman Filter (EKF), which is able to handle bad signal quality caused by shading or loss of Doppler Effect for low cost GNSS and IMU sensors fused in a loosely coupled way. It uses the estimated position error as well as the speed to calculate the standard deviation for the measurement uncertainty matrix of the Kalman Filter. The filter is very easy to implement, because some conversions of the measurement, as well as the state variables, are made to reduce the complexity of the Jacobians, which are used in the EKF filter algorithm. The filter implementation is tested within a simulation and with real data and shows significantly better performance, compared to a standard EKF. The developed filter is running in realtime on an embedded device and is able to perform position and attitude estimation of a vehicle with low cost sensors.**

***Index Terms*—Extended Kalman Filter, Adaptive, Position Estimation**

I. Introduction

The Kalman Filter is widely used in a lot of applications, since R.E. Kalman introduced it in 1960 [1]. A vast number of papers have been published about the Kalman Filter and its special variations for special problems. A lot of them adressing problems about sensor fusion for unmanned autonomous vehicles (e.g. [2]–[5]). Implementations with adaptive calculation of the measurment uncertainty matrices R and Q are presented (e.g. [6]). Some of them deal with different driving situations (dynamic vs. standing) and using interactive multimodel fusion filtering (e.g. [7], [8]). Some papers addressing problems with low cost sensors (e.g. [7], [9], [10]) and odometry to supplement GNSS under signal masking conditions such as tree foliage and urban canyons (e.g. [8]). Most of the papers using additional sensors, like cameras (e.g. [11], [12]), wheel revolution sensors (e.g. [8]) or lidar sensors (e.g. [12]) to get a better position estimation. In this paper, we present a novel and very easy to implement adaptive EKF, which only uses low cost GNSS sensor and an intertial measurement unit (acceleration, rotation, magnetometer) to perform very well in dynamic situations and in rest position of a car.

II. Fundamentals

A. Kalman Filter

As introduced in [1], the Bayesian tracking algorithm estimates the probability density function (PDF) of a systems state vector x_k, recursively. In one timestep k the system state evolves with the state transition equation

$$\boldsymbol{x}_{k+1} = g(\boldsymbol{x}_k, \boldsymbol{u}_k, \omega_k) \tag{1}$$

to the next state. The noise ω is assumed to be zero mean multivariate Gaussian white noise with covariance Q.

$$\omega_k \sim \mathcal{WN}(0, \boldsymbol{Q_k}) \tag{2}$$

The control input u drives the state. The measurement function

$$\boldsymbol{y}_k = h(\boldsymbol{x}_k, \nu_k) \tag{3}$$

maps the measurements to the state vector with measurement noise ν, which is as well assumed to be

$$\nu_k \sim \mathcal{WN}(0, \boldsymbol{R_k}) \tag{4}$$

with the measurement noise covariance matrix R.

B. Uncertainty Matrices

The matrices have different roles in the Kalman Filter. The matrix Q models the uncertainty, which superimpose the system model. The matrix R models the uncertainty associated with the measurements. The error covariance matrix P is the matrix, which is recalculated in the prediction as well as in the correction step, by the Kalman filter itself. It shows the uncertainty of the state estimate as a function of time. Therefore, the values in P should decrease over time.

C. Linearization

The Kalman Filter actually just works for linear states and measurements. Most of real life problems, like the one presented in this paper, are nonlinear, either on the dynamic or the measurement, or both. The theory behind is, that a nonlinear state or measurement can be estimated by a Taylor approximation. The partial derivative of the state and the measurement with respect to state vector x or control vector u is well known as the Jacobian.

$$J_A = \left.\frac{\partial g}{\partial \boldsymbol{x}}\right|_{\hat{\boldsymbol{x}}_k, \boldsymbol{u}_k} \tag{5}$$

$$J_G = \left.\frac{\partial g}{\partial \boldsymbol{u}}\right|_{\hat{\boldsymbol{x}}_k, \boldsymbol{u}_k} \tag{6}$$

$$J_H = \left.\frac{\partial h}{\partial \boldsymbol{x}}\right|_{\hat{\boldsymbol{x}}_k, \boldsymbol{u}_k} \tag{7}$$

D. Extended Kalman Filter

Both, the Uncented and the Extended Kalman Filter perform evenly well on nonlinear states, but like St. Pierre et. al. in [13] pointed out, the Extended Kalman Filter is significantly more efficient in computational time. Depending on the complexity of the state transition function (1) and measurement function (3), the EKF is up to 22x faster [13].

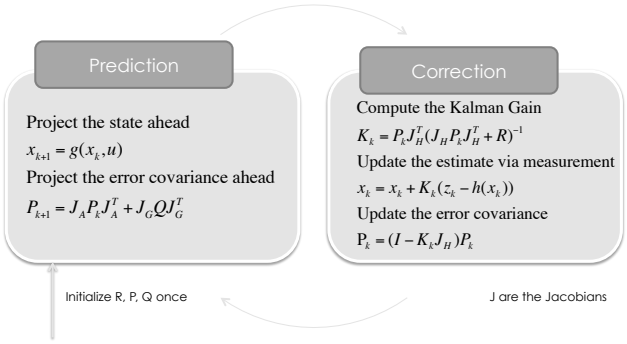

Fig. 1. Extended Kalman Filter Step

Because the computational time is an important fact for real time state estimation, the EKF presented in this paper uses some calculations/conversions before the EKF itself, to reduce the complexity of the Jacobians, especially for the measurement function h.

E. GNSS Position Accuracy

In this paper, an adaptive extended Kalman Filter is introduced, which recalculates the measurement noise uncertainty for the position, based on the estimated position error (EPE), which is calculated by the GNSS receiver itself.

As [14] wrote, "the EPE is a scalar indicating the precision of the receiver based on the deviation of the measurements from the mean of the measurement."

For this reason, it cannot be used to determine a bias in the position measurement of the GNSS, but its relative error.

$$EPE \sim \text{HDOP} \cdot \text{URA}(1\sigma) \tag{8}$$

With HDOP as the Horizontal Delution of Precision and URA as the User Range Accuracy, which is a quantity that is transmitted in the navigation message and that is the predicted (not measured) statistical ranging accuracy.

III. Extended Kalman Filter for CTRV dynamic with Attitude Estimation

The implemented EKF estimates following state vector x_k, which is well known as the constant turn rate and velocity (CTRV) vehicle model + roll and pitch estimation:

$$x_k = \begin{bmatrix} x \\ y \\ \psi \\ v \\ \dot{\psi} \\ \phi \\ \dot{\phi} \\ \Theta \\ \dot{\Theta} \end{bmatrix} = \begin{bmatrix} \text{Position X (GNSS)} \\ \text{Position Y (GNSS)} \\ \text{Heading (GNSS)} \\ \text{Speed (GNSS)} \\ \text{Yaw Rate (IMU)} \\ \text{Pitch (IMU)} \\ \text{Pitchrate (IMU)} \\ \text{Roll (IMU)} \\ \text{Rollrate (IMU)} \end{bmatrix} \tag{9}$$

As Schubert et. al. determined in [15], "for ego motion estimation purposes which are characterized by a high update rate and the observability of v and $\dot{\psi}$, model complexities beyond CTRV do not appear to be beneficial. However, the CTRV model shows its advantages as soon as a heading estimate is required." The coordinate system is defined as shown in Fig. 2.

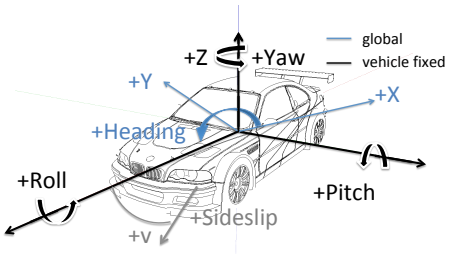

Fig. 2. Right hand coordinate system with z-axis to top

A. Roll and Pitch Angle

In [16], Madgwick presents an efficient orientation filter for inertial and inertial/magnetic sensor arrays. "The filter uses a quaternion representation, allowing accelerometer and magnetometer data to be used in an analytically derived and optimised gradient-descent algorithm to compute the direction of the gyroscope measurement error as a quaternion derivative.". The filter is implemented on the IMU and provides attitude information in quaternion representation in the global IMU coordinate system.

As mentioned there, the filter only estimates the correct attitude, if no external acceleration is actuating the vehicle. The calculated roll and pitch angles are actually just valid while standing still, not while accelerating/braking or cornering.

Madgwick recommended to adaptively choose convergence parameters, depending on absolute acceleration, influencing the IMU.

This paper lives this recommendation up and introduces an adaptively chosen weighting of roll and pitch angle and roll-/pitchrate, depending on the accelerations in x- or y-direction.

The roll and pitch angles, in vehicle coordinate system, are calculated with the quaternion ($Z_D = a - b\mathrm{i}_1 - c\mathrm{i}_2 - d\mathrm{i}_3$) output of the orientation filter [17].

$$\phi = -\arcsin(2 \cdot (a \cdot c - b \cdot d)) \tag{10}$$

$$\theta = -\arctan\left(\frac{2 \cdot (c \cdot d + a \cdot b)}{-(a^2 - b^2 - c^2 + d^2)}\right) \tag{11}$$

B. Position

The position x and y is determined with a low cost GNSS receiver. The conversion between WGS84 Lat and Lon degrees to SI units is calculated as follows: Assume the earth's radius with $R = 6378\,\mathrm{km}$, then one degree of Lon is

$$arc = \frac{2\pi \cdot R}{360°} = 111{,}323\,\mathrm{km/°} \tag{12}$$

One degree Lat is 111,32 km only near the equator. If moving to the poles, the value decreases until it is 0 km on North- or Southpole. Taking the cos of the Lat provides the correct length reduction (see Fig. 3).

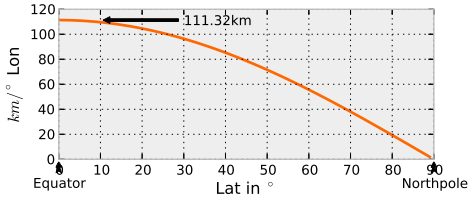

Fig. 3. Length of one degree of Longitude, depending on Latitude (WGS84)

$$\Delta x = arc \cdot \cos(Lat) \cdot \Delta Lon \tag{13}$$

$$\Delta y = arc \cdot \Delta Lat \tag{14}$$

With these equations the distance moved between two GNSS measurements can be calculated very accurate and additionally they simplify the state transition equations and the measurement function h, compared to other implementations, e.g. in [18].

C. State Control

The rollrate $\dot{\Theta}$, the pitchrate $\dot{\phi}$, the yawrate $\dot{\psi}$ as well as the speed v are state control variables.

$$u_k = \begin{bmatrix} v & \dot{\psi} & \dot{\phi} & \dot{\Theta} \end{bmatrix}^T \tag{15}$$

The vector u drives the state from one timestep k to the next one.

D. State Transition Function

The state transition function $g(x_k, u_k)$ is defined with

$$x_{k+1} = \begin{bmatrix} x + \frac{v}{\dot{\psi}}\left(-\sin(\psi) + \sin\left(T\dot{\psi} + \psi\right)\right) \\ y + \frac{v}{\dot{\psi}}\left(\cos(\psi) - \cos\left(T\dot{\psi} + \psi\right)\right) \\ T\dot{\psi} + \psi \\ v \\ \dot{\psi} \\ T\dot{\phi} + \phi \\ \dot{\phi} \\ T\dot{\Theta} + \Theta \\ \dot{\Theta} \end{bmatrix} \tag{16}$$

for $\dot{\psi} \neq 0$. For straight driving without curvature, the state transition function is

$$x_{k+1} = \begin{bmatrix} x + vT \cdot \cos(\psi) \\ y + vT \cdot \sin(\psi) \\ \psi \\ v \\ 0 \\ T\dot{\phi} + \phi \\ \dot{\phi} \\ T\dot{\Theta} + \Theta \\ \dot{\Theta} \end{bmatrix} \tag{17}$$

with T as the time between two filtersteps. The Jacobians of the state transition with respect to the state and w.r.t. the control are listed in appendix.

E. Process Noise Covariance Matrix Q

As Kelly in [19] pointed out "a Kalman filter is a mathematical idealization that happens to be useful in practice. However, it is important to note that there is a big difference between an optimal estimate and an accurate estimate. In practical use, the uncertainty estimates take on the significance of relative weights of state estimates and measurements. So it is not so much important that uncertainty is absolutely correct as it is that it be relatively consistent across all models."

$$Q = diag\begin{bmatrix} \sigma_v^2 & \sigma_{\dot{\psi}}^2 & \sigma_{\dot{\phi}}^2 & \sigma_{\dot{\Theta}}^2 \end{bmatrix} \tag{18}$$

Cross covariances resulting from deviation moments are assumed to be zero.

Assumptions for process noises for yawrate and velocity for a vehicle model are suggested in [19]. The process noise is best described with the question, how much the state can be propagated in one timestep by expected movement of the vehicle. So the maximal acceleration expected for a car might be $5\,\mathrm{m/s^2}$ under normal circumstances, so the $\sigma_v \approx a_{\max} \cdot T$. A typical maximal angular acceleration around vehicle z-axis might be $55\,°/\mathrm{s^2}$, which leads to a process noise of $\sigma_{\dot{\psi}} \approx 55\,°/\mathrm{s^2} \cdot \frac{\pi}{180,0} \cdot T$. The rotation around the pitch axis is much more dynamical, with typical angular accelerations of $200\,°/\mathrm{s^2}$. The rotation around the roll axis is in between and is assumed to be $130\,°/\mathrm{s^2}$. The process noises for a 50 Hz filter are listed in Table I.

TABLE I
PROCESS NOISE STANDARD DEVIATIONS

Parameter	Decribtion	Value
σ_v	Velocity Process Noise	0,1 m/s
$\sigma_{\dot{\psi}}$	Yawrate Process Noise	0,019 rad/s
$\sigma_{\dot{\phi}}$	Pitchrate Process Noise	0,07 rad/s
$\sigma_{\dot{\Theta}}$	Rollrate Process Noise	0,045 rad/s

F. Measurement Noise Covariance R

Because the estimation of roll (10) and pitch (11) is only valid for quasistatic situations (which is acutally not valid for a moving vehicle), the standard deviation for the calculated attitude angles σ_r are adaptive to the accelerations a_x and a_y.

The novel approach, presented in this paper, is the very easy to implement and fast to calculate weighting of the measurement noise covariance matrix R.

$$R = diag\begin{bmatrix}\sigma_x^2 & \sigma_y^2 & \sigma_\phi^2 & \sigma_\Theta^2\end{bmatrix} \tag{19}$$

1) Position Measurement Uncertainty: In every EKF filterstep, the standard deviations for σ_x and σ_y are calculated, depending on the speed and additionally depending on the estimated position error (EPE), which is provided by the GNSS modul itself.

$$\sigma_x^2 = \sigma_y^2 = \sigma_\mathrm{v}^2 + \sigma_\mathrm{EPE}^2 \tag{20}$$

with

$$\sigma_v = (v + \epsilon)^{-\xi} \tag{21}$$

$$\sigma_\mathrm{EPE} = \zeta \cdot EPE \tag{22}$$

The variables ϵ, ξ and ζ are tuneable parameters.

2) Attitude Measurement Uncertainty: The uncertainty for roll and pitch angle are adaptively calculated, depending on the vehicle accelerations in the appropriate directions.

$$\sigma_\Theta = (\rho + \gamma \cdot a_y)^2 \tag{23}$$

$$\sigma_\psi = (\rho + \gamma \cdot a_x)^2 \tag{24}$$

The variables ρ and γ are tuneable parameters.

G. Measurement Function h

Because of the simplifications (13) and (14), the Jacobian of the measurement function h with respect to the state x_k is simple and computationally fast with

$$J_H = \begin{bmatrix}1&0&0&0&0&0&0&0&0\\0&1&0&0&0&0&0&0&0\\0&0&0&0&0&1&0&0&0\\0&0&0&0&0&0&0&1&0\end{bmatrix} \tag{25}$$

when a new GNSS position measurement is available. In the practical implementation, the GNSS provide position information with 10,0 Hz and the EKF is estimating with 50,0 Hz. If no GNSS position information is available, the Jacobian of the measurement function h with respect to the state x_k is

$$J_H = \begin{bmatrix}0&0&0&0&0&0&0&0&0\\0&0&0&0&0&0&0&0&0\\0&0&0&0&0&1&0&0&0\\0&0&0&0&0&0&0&1&0\end{bmatrix} \tag{26}$$

IV. SIMULATION

A. Simulation Setup

To evaluate the adaptive EKF, a typical urban scenario, with shading from a buildings, as well as a vehicle stop, was simulated (see Fig. 4).

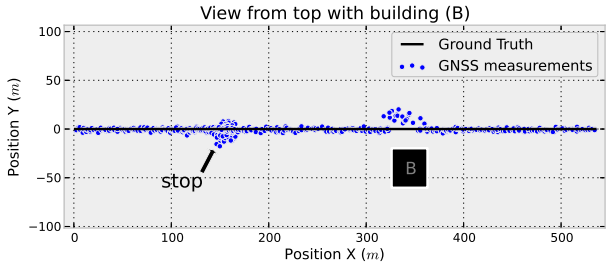

Fig. 4. Simulated GNSS measurements with vehicle stop and shading from a building (B) as well as ground truth

The car starts at $x = 0$, $y = 0$ with $v = 50{,}0$ km/h and decelerates until it stops. It is standing for 20 s and accelerating until it reaches $v = 50{,}0$ km/h again. Then it is passing a building, which disrupts the signal quality of the GNSS, so the position measurement is changed by $+15$ m in y-direction, the EPE is raised as well.

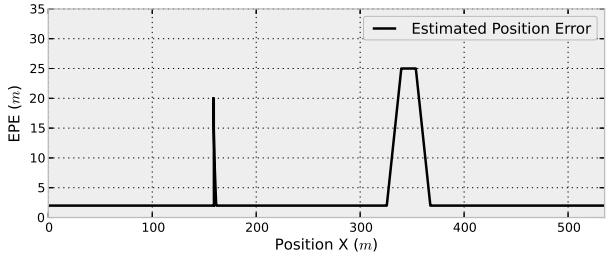

Fig. 5. Simulated GNSS Estimated Position Error

B. Parameter for Adaptive R

The summand ϵ for (21) is initialized with 1,0 m/s, the exponent ξ for (21) with 500,0 and the factor ζ for (22) with 50,0. The resulting values for σ_x^2 and σ_y^2 for a range of velocities and EPEs are shown in Fig. 6.

The factor ρ for (23) was initialized with 200,0, the summand γ was chosen to be 500,0.

These parameters are empirically chosen and are subject to change for different cars or other driving scenarios or street quality.

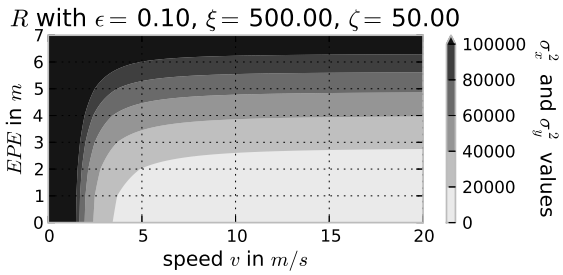

Fig. 6. Values of σ_x^2 and σ_y^2 in R, depending on v and EPE

C. Simulation Results

As one can see in Fig. 7, the filter follows the trajectory of the GNSS measurements. If the EPE raises, the filter is more willing to trust the control input (see (15)) instead of the position measurements.

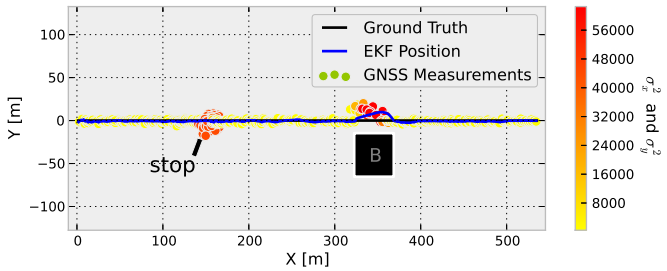

Fig. 7. Measurements of GNSS with color coded value for R, depending on speed and EPE as well as estimated trajectory of the EKF

To quantify the filter performance with respect to ground truth (GT) trajectory, the cross track error is introduced.

$$\text{CTE}_x = x_{GT} - x \tag{27}$$

$$\text{CTE}_y = y_{GT} - y \tag{28}$$

The sum of the square of the CTE for the simulation is a value to quantify the filter performance with respect to the correct trajectory estimation (see Fig. 8).

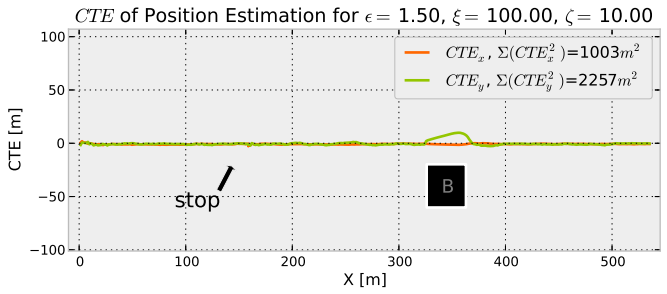

Fig. 8. Cross-Track-Error (not position estimate) with sum of the square

D. Comparison to Standard EKF

To compare the estimated trajectory with a non-adaptive EKF, the estimation was performed with several datasets for GNSS position measurements, generated by random Gaussian noise around the ground truth position.

The standard EKF was set up with static $\sigma_x^2 = 36\,\text{m}^2$ and $\sigma_y^2 = 36\,\text{m}^2$ values. The result is shown in Fig. 9.

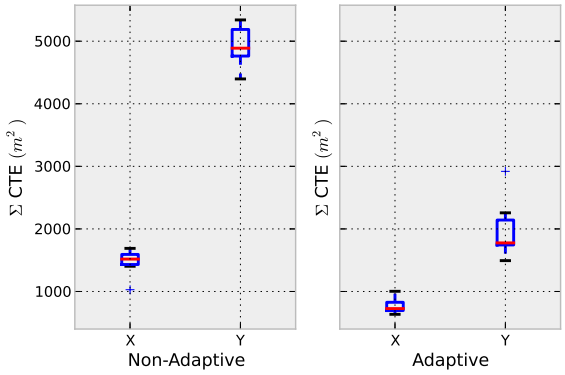

Fig. 9. Comparison of the mean, upper and lower quantile of several runs for trajectory estimation and values for sum of squares of the CTE for the adaptive and the standard EKF

In comparison, the adaptive EKF reduces the ΣCTE_x^2 by 47 %, the ΣCTE_y^2 by 59 %, which for sure depends on the driving direction as well as on the chosen parameters.

Note, that the standard EKF could set up with high values for R as well and may have better CTE values, but then, like for all filters, the dynamic is getting lost.

V. Experimental Setup

To test the performance of the filter with real GNSS data as well as a real car, the following sensores were used: LSM303 3-axis accelerometer and 3-axis magnetometer, ITG-3200 3-axis gyro, PA6H GNSS receiver. The sensors are available with the Tinkerforge IMU Brick[1] and GPS Bricklet[2].

For vehicle speed lower than 1,0 km/h (GNSS), the speed and yawrate are set to zero, because the Doppler effect doesn't work for speed estimation in the GNSS receiver and turning while standing still is very unlikely.

VI. Experimental Results

The state variables x_k for the scenario were estimated as shown in Fig. 11.

As one can see, the stop before the last left turn got a high position measurement uncertainty, which in detail is shown in figure 12.

The state variables for vehicle speed and yawrate are nearly perfectly aligned, because they fit very well and they are state control variables as well. The state is forced to follow them.

While standing still, the heading measurement of the GNSS receiver is inaccurate (see Fig. 11 between filter step $k \approx$

[1]http://www.tinkerforge.com/en/doc/Hardware/Bricks/IMU_Brick.html
[2]http://www.tinkerforge.com/en/doc/Hardware/Bricklets/GPS.html

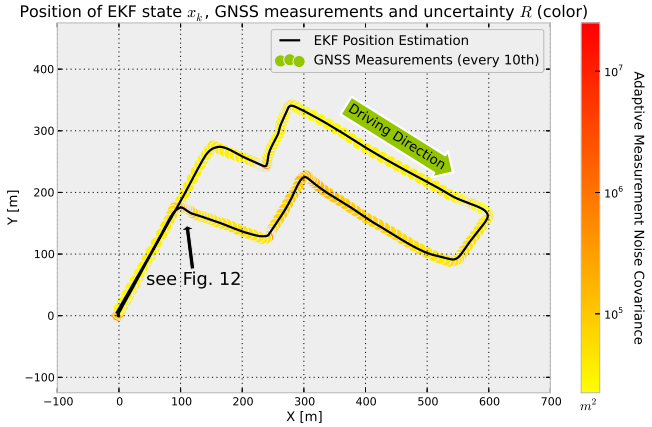

Fig. 10. Performed test drive with adaptive values of measurement uncertainty values for matrix R (color)

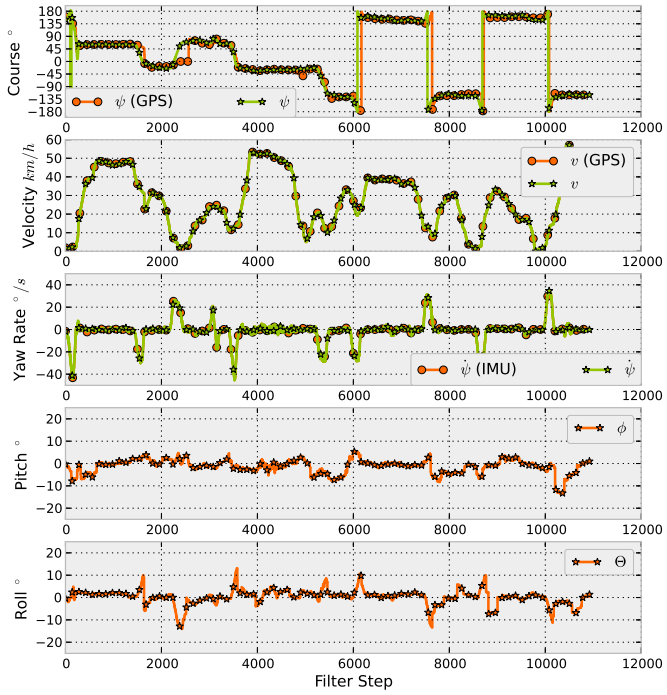

Fig. 11. Estimated state variables x_k for real world test drive

2100 . . . 2300). The filter performes very well on this situation and keeps the heading in the correct direction. The EKF position estimation (see Fig. 12) is not disturbed by inaccurate GNSS measurements while standing still and is dynamically responsive while driving.

For the conducted test drive, the values for the measurement uncertainties in R are calculated like shown in figure 13.

VII. Conclusion

In this paper we presented a novel approach to adaptively calculate the measurement uncertainty for an improved position and attitude estimation, based on the Estimated Position Error and the speed, determined by the low cost GNSS

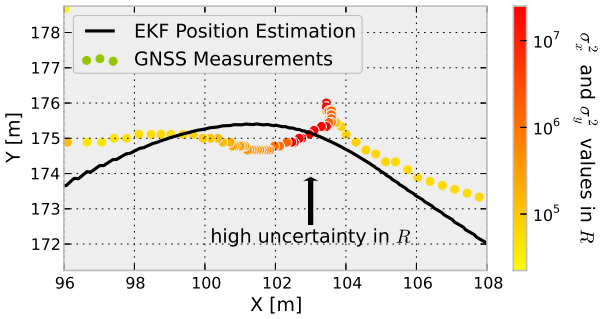

Fig. 12. Stop within the performed test drive with raised uncertainty for R and position estimation from adaptive EKF

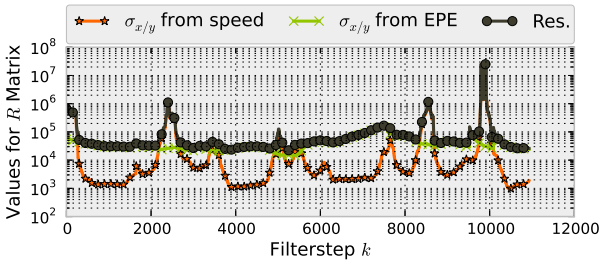

Fig. 13. Values for adaptive σ_v, σ_{EPE} and resulting σ for x and y

receiver. We explained the basics and used some empirically chosen values to parametrize the filter. With that, we showed with simulated data, that the filter performes significantly better than a standard Extended Kalman Filter. Based on that, we conducted test drives and used the developed Adaptive EKF for a real world dataset, which proved its ability to improve the position estimation with partly bad signal quality. In addition to that, the filter also performs pretty well on dynamic situations and is not loosing the ability to follow dynamic vehicle movements. The filter cannot be used to get rid of bias in position estimation, because the EPE from GNSS has, by definition, no information about static drift of the position information. The presented filter can be used to get significantly better results while standing still or driving slowly as well as keeping the heading fixed while do so. Additionally, the attitude of the vehicle is estimated, based on the filter presented in [16] in rest position and with angular velocity sensors from IMU while driving.

Acknowledgment

T.b.d.

Appendix A
Programm Code and EKF Implementation

The implemenented EKF code as well as all figures and the data used in this paper can be found online at t.b.d

APPENDIX B
JACOBIANS

The Jacobian of the state transition (16) function with respect to the state x_k is defined with

$$J_A = \begin{bmatrix} 1 & 0 & J_{A,13} & J_{A,14} & J_{A,15} & 0 & 0 & 0 & 0 \\ 0 & 1 & J_{A,23} & J_{A,24} & J_{A,25} & 0 & 0 & 0 & 0 \\ 0 & 0 & 1 & 0 & T & 0 & 0 & 0 & 0 \\ 0 & 0 & 0 & 1 & 0 & 0 & 0 & 0 & 0 \\ 0 & 0 & 0 & 0 & 1 & 0 & 0 & 0 & 0 \\ 0 & 0 & 0 & 0 & 0 & 1 & T & 0 & 0 \\ 0 & 0 & 0 & 0 & 0 & 0 & 1 & 0 & 0 \\ 0 & 0 & 0 & 0 & 0 & 0 & 0 & 1 & T \\ 0 & 0 & 0 & 0 & 0 & 0 & 0 & 0 & 1 \end{bmatrix} \tag{29}$$

with

$$J_{A,13} = \frac{v}{\dot{\psi}} \left(-\cos(\psi) + \cos\left(T\dot{\psi} + \psi\right)\right) \tag{30}$$

$$J_{A,14} = \frac{1}{\dot{\psi}} \left(-\sin(\psi) + \sin\left(T\dot{\psi} + \psi\right)\right) \tag{31}$$

$$J_{A,15} = \frac{Tv}{\dot{\psi}} \cos\left(T\dot{\psi} + \psi\right) - \frac{v}{\dot{\psi}} \cdot J_{A,14} \tag{32}$$

$$J_{A,23} = \frac{v}{\dot{\psi}} \left(-\sin(\psi) + \sin\left(T\dot{\psi} + \psi\right)\right) \tag{33}$$

$$J_{A,24} = \frac{1}{\dot{\psi}} \left(\cos(\psi) - \cos\left(T\dot{\psi} + \psi\right)\right) \tag{34}$$

$$J_{A,25} = \frac{Tv}{\dot{\psi}} \sin\left(T\dot{\psi} + \psi\right) - \frac{v}{\dot{\psi}} \cdot J_{A,24} \tag{35}$$

The Jacobian of the state transition function with respect to the control is

$$J_G = \begin{bmatrix} J_{G,11} & J_{G,12} & 0 & 0 \\ J_{G,21} & J_{G,22} & 0 & 0 \\ 0 & T & 0 & 0 \\ 1 & 0 & 0 & 0 \\ 0 & 1 & 0 & 0 \\ 0 & 0 & T & 0 \\ 0 & 0 & 1 & 0 \\ 0 & 0 & 0 & T \\ 0 & 0 & 0 & 1 \end{bmatrix} \tag{36}$$

with

$$J_{G,11} = \frac{1}{\dot{\psi}} \left(-\sin(\psi) + \sin\left(T\dot{\psi} + \psi\right)\right) \tag{37}$$

$$J_{G,12} = \frac{Tv}{\dot{\psi}} \cos\left(T\dot{\psi} + \psi\right) - \frac{v}{\dot{\psi}} \cdot J_{G,11} \tag{38}$$

$$J_{G,21} = \frac{1}{\dot{\psi}} \left(\cos(\psi) - \cos\left(T\dot{\psi} + \psi\right)\right) \tag{39}$$

$$J_{G,22} = \frac{Tv}{\dot{\psi}} \sin\left(T\dot{\psi} + \psi\right) - \frac{v}{\dot{\psi}} \cdot J_{G,21} \tag{40}$$

REFERENCES

[1] R. E. Kalman, "A New Approach to Linear Filtering and Prediction Problems," vol. 82, no. Series D, pp. 35–45, 1960. [Online]. Available: http://www.cs.unc.edu/~welch/kalman/media/pdf/Kalman1960.pdf

[2] I. Penarrocha and R. Sanchis, "Adaptive extended Kalman filter for recursive identification under missing data," *49th IEEE Conference on Decision and Control (CDC)*, pp. 1165–1170, 2010.

[3] A. Mourikis and S. Roumeliotis, "A Multi-State Constraint Kalman Filter for Vision-aided Inertial Navigation," *Proceedings 2007 IEEE International Conference on Robotics and Automation*, 2007.

[4] F. S. F. Sun, W. X. W. Xu, and J. L. J. Li, "Enhancement of the Aided Inertial Navigation System for an AUV via micronavigation," *OCEANS 2010*, 2010.

[5] M. Barczyk and A. F. Lynch, "Invariant Extended Kalman Filter design for a magnetometer-plus-GPS aided inertial navigation system," *IEEE Conference on Decision and Control and European Control Conference*, pp. 5389–5394, 2011.

[6] V. Bistrovs and A. Kluga, "Adaptive Extended Kalman Filter for Aided Inertial Navigation System." *Electronics & Electrical Engineering*, vol. 6, no. 6, 2012. [Online]. Available: http://eejournal.ktu.lt/index.php/elt/article/viewFile/1818/1476

[7] R. Toledo-Moreo, "High-integrity IMM-EKF-based road vehicle navigation with low-cost GPS/SBAS/INS," *Intelligent ...*, vol. 8, no. 3, pp. 491–511, 2007. [Online]. Available: http://ieeexplore.ieee.org/xpls/abs_all.jsp?arnumber=4298913

[8] J. Stephen and G. Lachapelle, "Development and Testing of a GPS-Augmented Multi-Sensor Vehicle navigation system," *The Journal of Navigation*, vol. 54, pp. 297–319, 2001.

[9] H. von Rosenberg, "Sensorfusion zur Navigation eines Fahrzeugs mit low-cost Inertialsensorik," Diplomarbeit, Universität Stuttgart, 2006.

[10] D. Kingston and R. Beard, "Real-Time Attitude and Position Estimation for Small UAVs Using Low-Cost Sensors," *AIAA 3rd "Unmanned Unlimited" Technical Conference, Workshop and Exhibit*, pp. 1–9, Sep. 2004. [Online]. Available: http://arc.aiaa.org/doi/abs/10.2514/6.2004-6488

[11] J. Effertz, "Autonome Fahrzeugführung in urbaner Umgebung durch Kombination objekt- und kartenbasierter Umfeldmodelle," Ph.D. dissertation, Technische Universität Carolo-Wilhelmina zu Braunschweig, 2009.

[12] V. von Holt, "Integrale multisensorielle Fahrumgebungserfassung nach dem 4D-Ansatz," Ph.D. dissertation, Universität der Bundeswehr München, 2004. [Online]. Available: http://ub.unibw-muenchen.de/dissertationen/ediss/holt-volker/meta.html

[13] M. St-Pierre and D. Gingras, "Comparison between the unscented Kalman filter and the extended Kalman filter for the position estimation module of an integrated navigation information system," *Intelligent Vehicles Symposium, 2004 ...*, 2004. [Online]. Available: http://ieeexplore.ieee.org/xpls/abs_all.jsp?arnumber=1336492

[14] M. Sharif and A. Stein, "Integrated approach to predict confidence of GPS measurement," *isprsserv.ifp.uni-stuttgart.de*, 2004. [Online]. Available: http://isprsserv.ifp.uni-stuttgart.de/proceedings/XXXV/congress/comm3/papers/344.pdf

[15] R. Schubert, C. Adam, M. Obst, N. Mattern, V. Leonhardt, and G. Wanielik, "Empirical evaluation of vehicular models for ego motion estimation," *2011 IEEE Intelligent Vehicles Symposium (IV)*, pp. 534–539, Jun. 2011. [Online]. Available: http://ieeexplore.ieee.org/lpdocs/epic03/wrapper.htm?arnumber=5940526

[16] S. Madgwick, "An efficient orientation filter for inertial and inertial/magnetic sensor arrays," *Report x-io and University of Bristol*, 2010. [Online]. Available: http://sharenet-wii-motion-trac.googlecode.com/files/An_efficient_orientation_filter_for_inertial_and_inertialmagnetic_sensor_arrays.pdf

[17] J. J. Buchholz, "Vorlesungsmanuskript Regelungstechnik und Flugregler," 2013. [Online]. Available: http://www.grin.com/de/e-book/82818/regelungstechnik-und-flugregler

[18] S. Wender, *Multisensorsystem zur erweiterten Fahrzeugumfelderfassung*, 2008. [Online]. Available: http://vts.uni-ulm.de/docs/2008/6605/vts_6605_9026.pdf

[19] A. Kelly, "A 3D state space formulation of a navigation Kalman filter for autonomous vehicles," no. May, 1994. [Online]. Available: http://oai.dtic.mil/oai/oai?verb=getRecord&metadataPrefix=html&identifier=ADA282853